Journal of Coordination Chemistry

ISSN: 0095-8972 (Print) 1029-0389 (Online) Journal homepage: http://www.tandfonline.com/loi/gcoo20

Synthesis, DNA binding and docking studies of copper(II) complexes containing modified phenanthroline ligands

J. Lakshmipraba, S. Arunachalam, R. Vijay Solomon & P. Venuvanalingam

To cite this article: J. Lakshmipraba, S. Arunachalam, R. Vijay Solomon & P. Venuvanalingam (2015) Synthesis, DNA binding and docking studies of copper(II) complexes containing modified phenanthroline ligands, Journal of Coordination Chemistry, 68:8, 1374-1386, DOI: 10.1080/00958972.2015.1014349

To link to this article: http://dx.doi.org/10.1080/00958972.2015.1014349

Accepted author version posted online: 04 Feb 2015.
Published online: 05 Mar 2015.

Journal of Coordination Chemistry, 2015
Vol. 68, No. 8, 1374–1386, http://dx.doi.org/10.1080/00958972.2015.1014349

Synthesis, DNA binding and docking studies of copper(II) complexes containing modified phenanthroline ligands

J. LAKSHMIPRABA, S. ARUNACHALAM*, R. VIJAY SOLOMON and P. VENUVANALINGAM

School of Chemistry, Bharathidasan University, Tiruchirappalli, India

(*Received 24 July 2014; accepted 9 January 2015*)

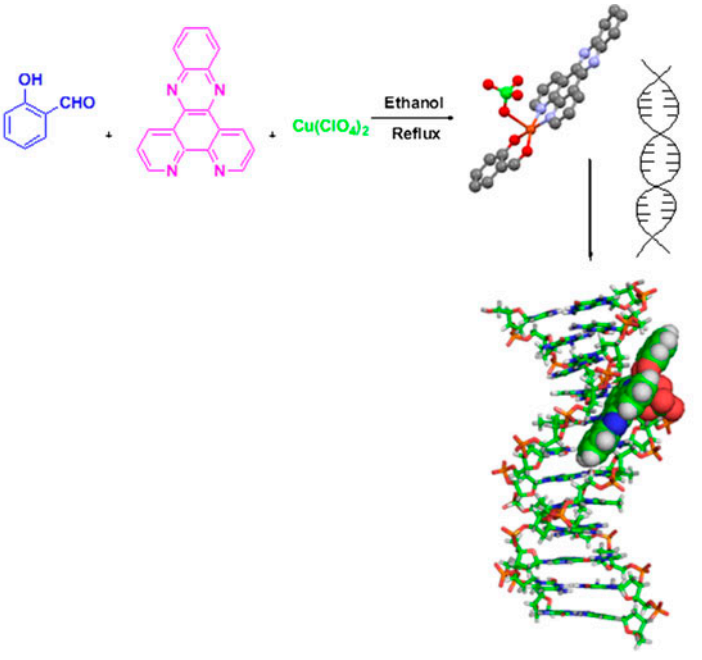

Copper(II) complexes, [Cu(Hsal)(L)(ClO_4)] (where Hsal = salicylaldehyde, **1**: L = dpqC = dipyrido[3,2-a:2′,3′-c](6,7,8,9-tetrahydro)phenazine and **2**: L = dppz = dipyrido[3,2-a:2′,3′-c]phenazine), were synthesized and characterized using elemental analysis and spectroscopic methods. Single-crystal XRD on **1** confirms the presence of square pyramidal geometry around Cu(II). DNA interaction studies were performed for both the complexes using UV–visible, fluorescence and circular dichroism spectroscopic techniques, and viscosity. These complexes bind with DNA through partial intercalation. Molecular docking studies confirm our experimental findings of mode of binding of our complexes with DNA.

Keywords: Copper complex; DNA binding; Molecular docking

*Corresponding author. Email: arunasurf@yahoo.com

1. Introduction

Structure–activity relationships of compounds showing photochemotherapeutic activity are important to enhance the biological activity of the molecules by modifying various structural and/or functional parameters, viz. steric and electronic controls, lipo- and hydrophilicity, and stability of molecules derived from the parent drug by suitable modification of substituent(s) [1]. Cisplatin is a widely used metal-based anticancer drug [2–4], but it is curative only in some selected tumors and due to side effects as well as acquired cellular resistance, its use is limited. So, the development of more efficacious, less toxic, and target-specific non-covalent DNA binding anticancer drugs has received attention. Generally, anticancer agents approved for clinical use are molecules which damage DNA, block DNA synthesis indirectly through inhibition of nucleic acid precursor biosynthesis or disrupt hormonal stimulation of cell growth [5]. Considerable efforts have been focused on the development of new anticancer drugs based on transition metal complexes. Copper is a bioessential element, which plays a key role in biological processes and its complexes are preferred molecules for anticancer inhibition [6]. It has been demonstrated that copper accumulates in tumors due to selective permeability of cancer cell membranes to copper compounds [7]. A number of copper(II) complexes have been screened for anticancer activity and some of them were active *in vitro* and *in vivo* [8, 9]. Porphyrin-, phthalocyanine- and other macrocyclic-based photodynamic therapy (PDT) agents have been designed to show strong correlations between the hydrophobicity of the PDT agents and their therapeutic activity [10–16]. Among metal-based PDT agents, rhodium, ruthenium, and iron complexes show strong dependence of biological activity on their molecular structures [17–20]. Extended planar aromatic ring in the ligands allows better intercalation with DNA [21].

We have synthesized two copper(II) complexes, $[Cu(Hsal)(L)(ClO)_4]$ (where L = dpqC and dppz). To study the structure–activity relationship of these complexes, we have prepared copper(II) complexes using modified phenanthroline ligands with increased aromatic surface using dipyridophenazine (dppz) and reducing the aromatic surface area by attaching a dearomatized cyclohexyl ring (dpqC). The characterizations of the complexes were done using analytical and spectral (IR, UV–vis, EPR) methods. X-ray diffraction studies were also carried out for **1** to determine the binding mode of the ligand in the complexes and the geometry of the complex. Studies on DNA binding of these complexes were performed using spectroscopic techniques and viscosity method. To gain further insights into the nature of DNA binding of these complexes, molecular docking calculations were performed and compared with experimental observations.

2. Experimental

2.1. *Materials*

Calf thymus DNA and copper(II) perchlorate hexahydrate were obtained from Sigma–Aldrich, Germany. Salicylaldehyde and 1,10-phenanthroline were purchased from Merck, India. dpqC and dppz are synthesized using literature methods [22, 23]. A solution of calf thymus DNA in the buffer gave a ratio of UV absorbance at 260 and 280 nm of ~1.8–1.9:1, indicating that the DNA was sufficiently free of protein. DNA binding experiments were performed at 25.0 ± 0.2 °C. DNA concentration per nucleotide was determined using

electronic absorption spectroscopy with the known molar extinction coefficient value of 6600 M^{-1} cm^{-1} for DNA [24]. All experiments involving the interaction of copper(II) complexes with DNA were carried out with double-distilled water in a buffer containing 5 mM Tris–HCl/50 mM NaCl: ethanol (100:1 v/v) at pH 7.1.

2.2. *Physical measurements*

Microanalyses (carbon, hydrogen, and nitrogen) of samples were performed at SAIF, Lucknow, India. Absorption spectra were recorded on a UV–vis–NIR Cary300 spectrophotometer using cuvettes of 1 cm path length, and emission spectra were recorded on a JASCO FP 770 spectrofluorimeter. FT-IR spectra were recorded on a FT-IR JASCO 460 PLUS spectrophotometer with samples prepared as KBr pellets. EPR spectra were recorded on a JEOL-FA200 EPR spectrometer in methanol at 77 K and in solid form at room temperature. Conductivity studies were done in aqueous solutions of the complexes with an Elico conductivity bridge type CM 82 and a dip-type cell with a cell constant of 1.0.

Absorption titration experiments of copper(II) complexes in buffer (50 mM NaCl–5 mM Tris–HCl, pH 7.1) were performed using a fixed complex concentration to which increments of the nucleic acid stock solutions were added. Copper(II) complex–nucleic acid solutions were allowed to incubate for 10 min before the absorption spectra were recorded. Equal solution of nucleic acid was added to both complex solution and reference solution to eliminate the absorbance of nucleic acid itself. For fluorescence quenching experiments, nucleic acids were pretreated with ethidium bromide (EB) for 30 min. Copper(II) complexes were then added to this mixture and their effect on emission intensity was measured. Samples were excited at 450 nm and emission was observed between 500 and 700 nm. Circular dichroic spectra were recorded at room temperature using the same Tris buffer. Viscosity experiments were carried out using an Ubbelodhe viscometer maintained at 25.0 ± 0.2 °C. DNA solutions were prepared by sonicating in order to minimize complexities arising from nucleic acid flexibility.

2.3. *Synthesis of [Cu(Hsal)(L)(ClO_4)]*

Copper(II) complexes were synthesized using the following general procedure: To a warm ethanolic solution (10 mL) of salicylaldehyde (0.20 mM), an ethanolic solution (10 mL) of $Cu(ClO_4)_2{\cdot}6H_2O$ (0.20 mM) was added followed by an ethanolic solution of L (dpqC or dppz) (0.20 mM) and stirred under reflux for 5–6 h. At the end of the reaction, the solution was filtered, the filtrate was reduced to half its volume and then kept for slow evaporation at room temperature whereby the complexes separated (scheme 1).

Complex **1** (L = dpqC): Yield: 73%; Anal. Calcd for $C_{25}H_{19}ClCuN_4O_6$ (570.43 g M^{-1}): C, 52.45; H, 3.70; N, 9.79; O, 16.77; Cu, 11.10%. Found: C, 52.59; H, 3.68; N, 9.78; O, 16.75; Cu, 11.09%. Selected IR data (KBr, cm^{-1}) 1518, 1332, 1265, 849, 726. UV–vis (ethanol, λ_{max} (ε (M^{-1} cm^{-1}))) 256 (42,740), 324 (11,250), 397 (1800), 696 (180). Conductance: 15 S cm^2 M^{-1}.

$$\mathrm{Hsal + L + Cu(ClO_4)_2{\cdot}6H_2O} \xrightarrow[\text{Reflux}]{\text{EtOH}} \mathrm{[Cu(sal)(L)(ClO_4)]}$$

(L = dpqC, dppz)

Scheme 1. Formation of complexes.

Complex **2** (L = dppz): Yield: 70%; Anal. Calcd for $C_{34}H_{26}Cl_2Cu_2N_4O_{12}$ (565.01 g M^{-1}): C, 53.01; H, 2.67; N, 9.89; O, 16.95; Cu, 11.22%. Found: C, 53.00; H, 2.64; N, 9.87; O, 16.96; Cu, 11.19%. Selected IR data (KBr, cm^{-1}) 1517, 1331, 1268, 850, 727. UV–vis (ethanol, λ_{max} (ε (M^{-1} cm^{-1}))): 255 (57,630), 322 (15,160), 391 (2410), 699 (240). Conductance: 17 S cm^2 M^{-1}.

2.4. *X-ray crystallography*

Blue prismatic single crystals of [Cu(Hsal)(dpqC)(ClO_4)] (**1**) were grown by slow evaporation of ethanol solution at room temperature. Data collection was carried out using a Bruker AXS Kappa APEX II single-crystal X-ray diffractometer using monochromated Mo K_α radiation (λ = 0.71073 Å). Data were collected at 293 K. Absorption corrections were performed using multi-scan method using SADABS [25]. Corrections were made for Lorentz and polarization effects. Structures were solved using direct methods (SHELXS 97) and refined using full-matrix least squares on F^2 using SHELXL 97 [26]. All non-hydrogen atoms were refined anisotropically and the hydrogens in these structures were located from the difference Fourier map and constrained to ideal positions in the refinement procedure. Unit cell parameters were determined using the method of difference vectors using reflections scanned from three different zones of the reciprocal lattice. Intensity data were measured using ω and φ scan with a frame width of 0.5°. Frame integration and data reduction were performed using the Bruker SAINT-Plus (Version 7.06a) software [27]. The crystallographic data of **1** are given in table 1 and selected bond lengths and angles relevant to copper coordination sphere are collected in table 2.

Table 1. Crystal data and structure refinement for [Cu(Hsal)(dpqC)(ClO_4)] (**1**).

Empirical formula	$C_{25}H_{19}ClCuN_4O_6$
Formula weight	570.43
Temperature (K)	293(2) K
Radiation type	MoKα
Wavelength (Å)	0.71073
Crystal system	Monoclinic
Space group	*P21/c*
a (Å)	16.3607(6)
b (Å)	9.1570(3)
c (Å)	17.6926(7)
α (°)	90.00
β (°)	117.54
γ (°)	90.00
Volume ($Å^3$)	2350.29(15)
Z	4
Calculated density (Mg m^{-3})	1.612
Absorption coefficient (mm^{-1})	1.094
F(0 0 0)	1164
Crystal size (mm)	0.09 × 0.06 × 0.06
Theta range (°)	2.58–27.17
Limiting indices	$-20 \le h \le 20$, $-11 \le k \le 11$, $-22 \le l \le 16$
Reflections collected/unique	4074/14,581
Refinement method	Full-matrix least squares on F^2
Data/restraints/parameters	14,581/0/334
Goodness-of-fit on F^2	0.836
Final *R* indices [$I > 2\sigma(I)$]	R_1 = 0.0514, wR_2 = 0.1195
R indices (all data)	R_1 = 0.1150, wR_2 = 0.1375
Largest diff. peak and hole (e $Å^{-3}$)	0.001 and 0.000

Table 2. Selected bond lengths (Å) and angles (°) for **1**.

Bond lengths (Å)		Bond angles (°)	
Cu1–O1	1.937(3)	O1–Cu1–O2	95.19(16)
Cu1–O2	1.874(4)	O1–Cu1–O3	89.58(14)
Cu1–O3	2.472(4)	O1–Cu1–N1	90.33(14)
Cu1–N1	1.982(4)	O1–Cu1–N2	167.39(14)
Cu1–N2	2.014(3)	O2–Cu1–O3	95.24(16)
		O2–Cu1–N1	172.20(17)
		O2–Cu1–N2	91.27(16)
		O6–Cu1–N1	90.30(13)
		O6–Cu1–N2	100.62(13)
		N1–Cu1–N2	82.29(13)

Note: ESD in parenthesis.

2.5. *Computational details*

The geometries of both complexes were optimized at B3LYP/LANL2DZ level using G09W program [28]. Frequency analysis shows that they are minima in the potential energy surface. Computed bond parameters were compared with available crystal structures and there is excellent agreement between optimized geometry and its crystal structures. These optimized structures were further considered for molecular docking analysis using HEX 6.3, an interactive protein docking and molecular superposition program that is mainly used for feasible docking of various ligands with proteins, enzymes, DNA, and also in protein–protein docking [29]. Docking parameters were set to include ligand–DNA interactions and various parameters for non-covalent interactions were used as implemented in the program. The duplex DNA d(CGCGAATTCGCG)$_2$ dodecamer was taken from the Protein Data Bank (PDB ID: 355D) and used in docking studies. All possible docking poses were considered and the docking was performed.

3. Results and discussion

3.1. *Characterization*

3.1.1. Description of the crystal structure of 1. Complex **1** crystallized in the monoclinic lattice with a space group *P21/c*. The ORTEP representation of **1** including the atom numbering scheme is shown in figure 1. The crystallographic asymmetric unit of **1** contains square pyramidal geometry with a CuN_2O_3 coordination sphere. The nitrogens of dpqC and the carbonyl O1 and phenolate O2 of salicylaldehyde form the basal plane. The Cu–N distances observed [Cu1–N1, 1.982(4) Å; Cu1–N2, 2.014(3) Å] fall within the range of Cu–N imine distances observed for other diimine complexes [30–33]. The Cu–N1 bond (*trans* to the Cu–O2 phenolate bond) is slightly shorter than the Cu–N2 bond. Also, the Cu–O2 phenolate bond distance of 1.874(4) Å is shorter than that of Cu–O1 bond (1.937(3) Å), as expected. Perchlorate oxygen occupies the axial position. As shown in figure 2, intermolecular interaction between the perchlorate oxygen and metal center results in the formation of a zigzag arrangement which is likely to contribute to packing stabilization.

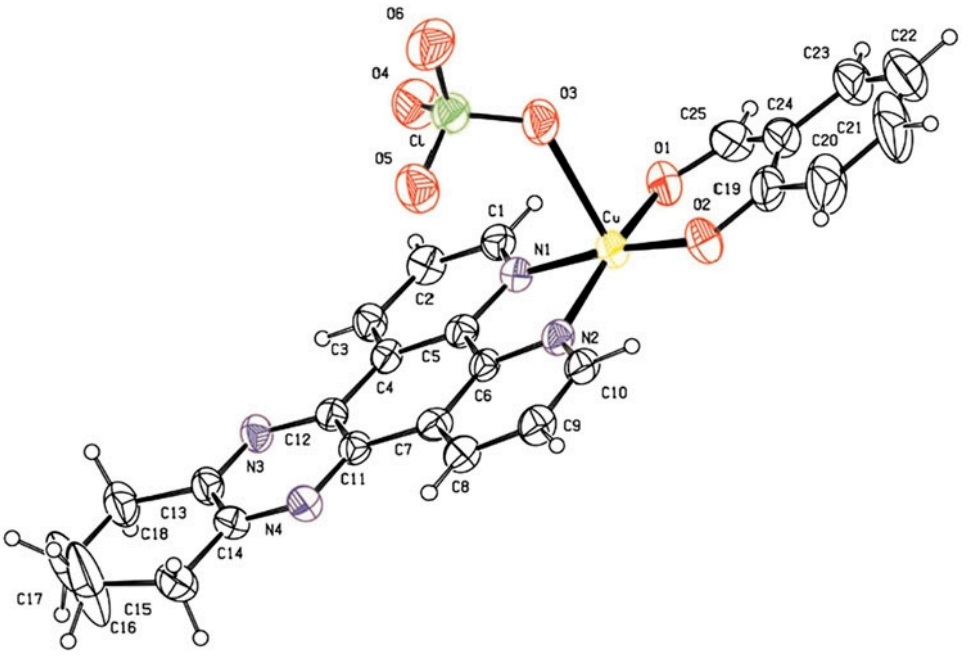

Figure 1. ORTEP diagram of [Cu(Hsal)(dpqC)(ClO_4)] (**1**) with the atoms represented as 30% anisotropic ellipsoids.

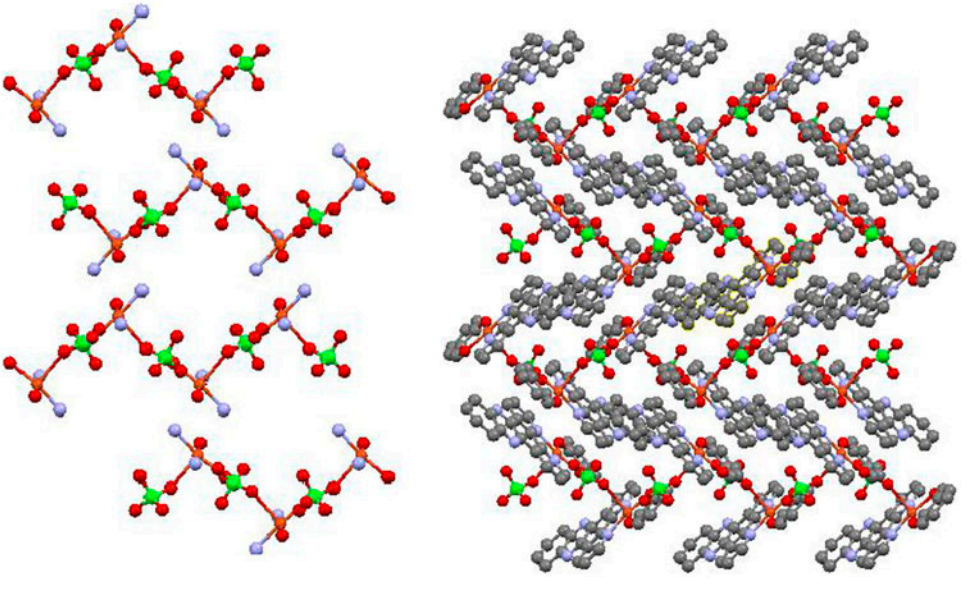

Figure 2. Fragment of the molecular packing and crystal packing diagram of **1** along the *a* axis.

Cu(II) has square pyramidal coordination formed using the two oxygens of salicylaldehyde (phenolate and carbonyl oxygens), the two diimine nitrogens of the dpqC, and a perchlorate ion. The τ factor defined for five-membered coordination spheres [34, 35] is given as $\tau = (\beta - \alpha)/60$, where β and α correspond to two largest angles around the metal. If $\tau = 0$ the coordination is an ideal square pyramid and if $\tau = 1$ the coordination is an ideal trigonal bipyramid. If the values listed in molecular geometry are employed, the τ value for **1** is 0.08, indicating that Cu(II) has a near-ideal square pyramidal geometry.

3.1.2. Spectral characterization of copper(II) complexes. All the complexes are non-hygroscopic and air stable in solution and in the solid state at room temperature. They are soluble in water producing intense blue solutions. None of the complexes is electrically conductive in solution. In the IR spectra of the complexes, the ν_{C-N} of phenanthroline (1558 cm^{-1}) and ν_{C-H} ring frequency (852 and 735 cm^{-1}) was red shifted to ~1518, ~852 and ~727 cm^{-1}, respectively, which indicates diimines (dppz and dpqC) are coordinated to copper through nitrogen [36]. In FT-IR spectra, the disappearance of the ν_{O-H} band (~3440 cm^{-1} for free Hsal) in the complexes indicates the deprotonation of the phenolic proton prior to coordination. Also, the band due to carbonyl oxygen (~1625 cm^{-1}) shows a modest decrease in the stretching frequency when compared to that of free Hsal (1518 cm^{-1}), indicating coordination of the carbonyl oxygen [37]. The UV–visible absorption spectra of all the complexes show two bands below 330 nm which are due to π–π* and n–π* transitions. The presence of the PhO− to Cu(II) ligand-to-metal charge transfer transition as an intense band at 391–397 nm in the complexes reveals involvement of the phenolate oxygen in coordination in solution. The weak band at ~700 nm is due to d–d transition of square pyramidal copper(II) complexes. EPR spectra of both the complexes at room temperature showed a single isotropic feature with $g_{iso} = 2.05$ (for **1**) and 2.07 (for **2**) and in frozen solution (77 K, in methanol) exhibited a typical four-line spectral pattern, with a $g_{\|}$ of 2.230 (for **1**), 2.234 (for **2**) and $g_{\perp}$ of 2.03 (for **1**), 2.05 (for **2**). Considering the similarities in the physical and spectral properties of both complexes, analogous molecular structure is conjectured for both complexes.

3.2. *UV–visible absorption spectral titrations*

UV–visible spectral studies provide preliminary information regarding the binding behavior between DNA and small molecules. The concentration of the complex was kept constant and DNA was added to that solution in increasing amounts. Generally, when metal complexes bind with DNA, if hypochromism with red shift in the absorption spectrum of the complex is observed, it indicates an intercalative mode involving a strong stacking interaction between the complex and the base pairs of DNA, whereas a non-intercalative mode of interaction shows hyperchromism with blue shift [38]. In the presence of DNA, the spectrum of **1** and **2** shows hyperchromism and a slight red shift (figure 3). This indicates that the complexes bind via partial intercalation. The extent of binding was calculated using the equation [39] $[DNA]/(\varepsilon_a - \varepsilon_f) = [DNA]/(\varepsilon_b - \varepsilon_f) + 1/K_b(\varepsilon_b - \varepsilon_f)$, where [DNA] is the concentration of DNA expressed in base pairs; ε_a, ε_f, and ε_b are the extinction coefficients of the apparent, free, and fully bound copper(II) complex, respectively, and K_b is the binding constant. A plot of $[DNA]/(\varepsilon_b - \varepsilon_f)$ *versus* [DNA] gives the binding constants, K_bs, as the ratio of slope to intercept. The K_bs thus obtained are shown in table 3. These values suggest that **2** binds with DNA more strongly than **1**. The reason for a stronger binding

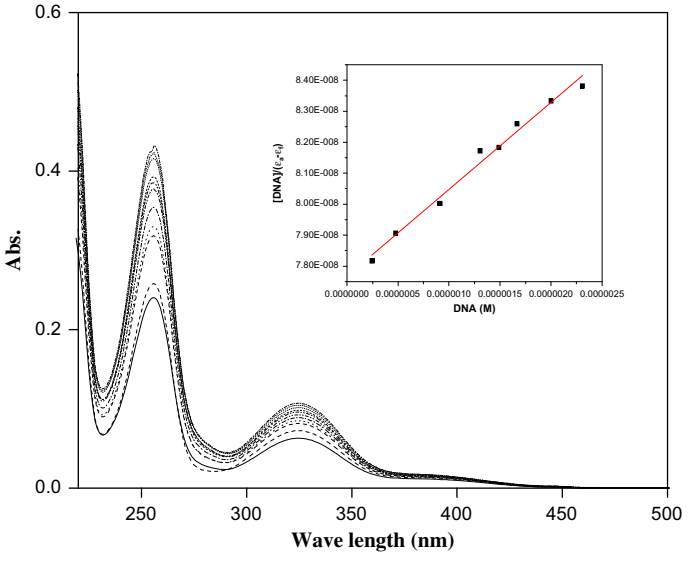

Figure 3. Absorption spectra of **2** [cpx] = 25 μM at increasing concentrations, 0–75 μM.

Table 3. Binding constant and quenching constant for **1** and **2** with DNA.

Complexes	$K_b \pm 0.01$ (M^{-1})	$K_{sv} \times 10^2$
1	2.42×10^3	1.2
2	4.08×10^4	2.5

constant of **2** is due to the extent of aromatic ring in **2** which is not present in **1**. The K_b of the present complexes suggests that these complexes bind with DNA with an affinity less than that of the classical intercalators [40, 41]. The K_b value is lower than those reported for typical classical intercalators (e.g. EB K_b ~10^6 M^{-1}) [42] and the partially intercalating complexes like $[Co(phen)_2(dppz)]^{3+}$ ($K_b = 9.09 \times 10^5$ M^{-1}) [43] and $[Ru(imp)_2(dppz)]^{2+}$ ($K_b = 2.19 \times 10^7$ M^{-1}, where imp = imidazo[4,5-f][1,10]-phenanthroline) [44], which implies that these complexes bind with DNA relatively less strongly than classical intercalators and partial intercalators. Generally, salicylaldehyde metal complexes bind via partial intercalators and are not expected to be classical intercalators [45, 46].

3.3. *EB competitive binding studies*

All the complexes are non-emissive. Therefore, EB fluorescence displacement experiments were conducted. The fluorescence intensity of EB in Tris buffer is not high due to quenching by solvent molecules. However, on addition of nucleic acid, the fluorescence intensity of EB is enhanced due to intercalation with DNA [47, 48]. The addition of a second molecule that binds with nucleic acid decreases the binding sites of DNA available for EB. In competitive binding studies, EB-pretreated DNA was excited at 450 nm and the emission was observed at 595 nm. On adding our complexes, there is a decrease in emission intensity

of EB-pretreated DNA adduct at 595 nm due to the replacement of EB-bound DNA by the complexes (figure 4). This decrease in the intensity at 595 nm shows semi-intercalation (partial intercalation) binding between DNA and our complexes. The quenching behavior can be analyzed through the Stern–Volmer equation, $I_0/I = 1 + K_{sv}r$, where I_0 and I are the fluorescence intensities in the absence and presence of complex, respectively, K_{sv} is the linear Stern–Volmer quenching constant, and r is the ratio of the total concentration of complex to that of nucleic acid. A plot of I_0/I *versus* [complex]/[DNA] is drawn, K_{sv}s are obtained from the ratio of slope to intercept. The quenching constants (K_{sv}) were calculated. These constants indicate that the quenching ability is **2** > **1**.

3.4. *Circular dichroism spectral studies*

Circular dichroism spectral studies are sensitive to conformational changes in DNA [49]. Generally no significant changes in the CD spectrum were observed for electrostatic and groove binders because these binding modes do not influence the secondary structure of DNA. The intercalating or partial intercalating molecules influence the secondary structure of DNA and the spectrum shows an increase in intensity with a blue or red shift [50, 51]. In our case, the CD spectrum of B-DNA shows a positive band at 273 nm and a negative band at 245 nm due to base stacking and right-handed helicity. On adding copper(II) complexes, the CD intensity of both positive and negative bands is increased (figure 5). This indicates that both the complexes bind with DNA through partial intercalation.

3.5. *Viscosity experiments*

Though spectroscopic techniques described above are widely used to study the binding mode of metal complexes with DNA, they do not give sufficient clues to support a binding model. Therefore, viscosity measurements were carried out to further clarify the nature of interaction of complexes with DNA. The classical intercalating molecules damage the DNA

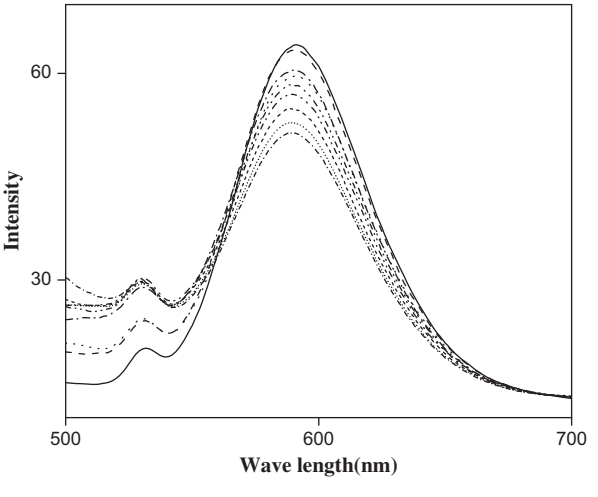

Figure 4. Emission spectra of EB-bound DNA ([EB] = 2 μM, [DNA] = 20 μM) with increasing concentrations of **2**, 0–49 μM.

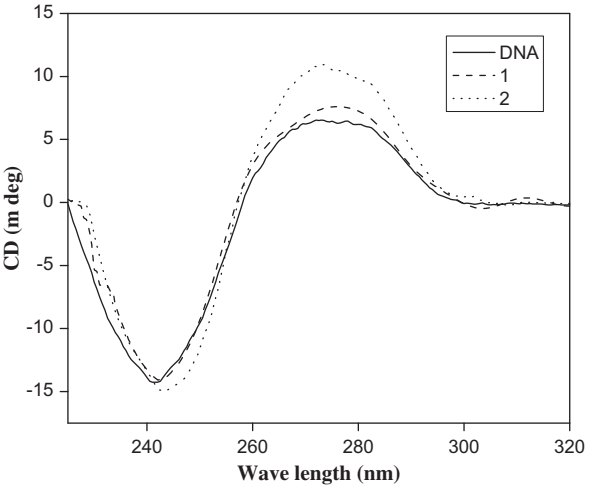

Figure 5. Circular dichroism spectra in the absence and presence of complexes, [DNA] = 40 μM and [**1** or **2**] = 60 μM.

double helix and lead to lengthening of the DNA. Non-intercalating complexes kink the DNA and reduce its viscosity [52]. In our case, DNA concentration was kept constant and adding the complexes to the solution, the viscosity of the DNA solution increased steadily (figure 6). Complex **2** shows almost equal viscosity similar to that of EB. This is due to the extent of aromatic ring present in the dppz ligand which binds via partial intercalation with DNA double helix, which was not present in **1**.

3.6. *Molecular docking analysis*

Both complexes have maintained a square pyramidal geometry with two nitrogens of dpqC/dppz and two oxygens of salicylaldehyde in the same plane. As expected, the axial Cu−O

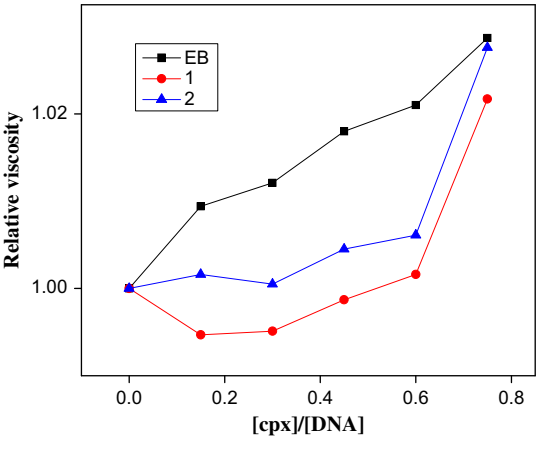

Figure 6. Effect of increasing amounts of EB, **1,** and **2** on the relative viscosity of DNA at room temperature. [Complex] = 45 μM.

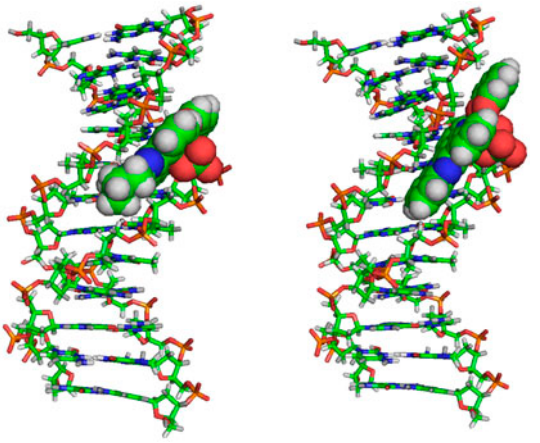

Figure 7. Molecular docking view of **1** and **2** with DNA.

(perchlorate) distances are longer, as a result of the Jahn–Teller distortion. Possible binding modes of ligands with DNA can be identified using docking analysis. Therefore, molecular docking studies were carried out with HEX 6.3 package and the energetically most probable docked poses are given in figure 7. Both complexes bind with DNA in an intercalative fashion near the minor groove. The perchlorate group has interactions with the backbone phosphate. Due to steric clash, the dpqC part of **1** is pushed outside of the base pairs and this leads to relatively poor binding as observed in experiments. At the same time, **2** shows a higher binding ability toward DNA due to its perfect planar structure. The dppz part of the complex perfectly fits into the available space between the strands and thereby leads to strong binding. Docking analysis shows that **2** has binding energy of 19.2 cal M^{-1} and seems to have a better binding ability compared to **1** and the order of binding of the complexes is **2** > **1** and well corroborated the experiments. In both cases, the metal complexes bind between the two strands and allow their whole molecule to interact with the DNA bases in intercalation. The planarity of the complex facilitates binding of these complexes via partial intercalation with DNA. Thus, our molecular modeling studies throw light on the binding modes through which these complexes interact with DNA and further support the experimental observations.

4. Conclusion

Copper(II) complexes containing ligands with extended aromatic rings and salicylaldehyde have been synthesized and characterized using spectroscopic and elemental analysis. **1** was characterized using the X-ray crystallographic technique. Studies have been done to know the binding of these complexes with DNA. Absorption and emission studies show that the complex binds with DNA via partial intercalation. Circular dichroism spectral studies suggest complexes with extended phenanthroline rings are involved in this partial intercalation. Viscosity experiments also suggest that both the complexes bind with DNA through partial intercalation. The binding strength of the complexes

follows the order **2** > **1**. Molecular docking studies also revealed the complexes show the same order of binding ability with DNA. Docking studies further indicate that both complexes bind with DNA through partial intercalation as observed in the experiments. The results show that the complexes bind with DNA and the ligand plays a key role in the process of DNA binding, indicating the potential utility of these complexes in the study of anticancer and antiviral drugs.

Supplementary material

Electronic supplementary information (ESI) available: CCDC reference number 838260 (for **1**).

Acknowledgements

We are grateful to the UGC-SAP and DST-FIST programmes (Bruker Smart APPEX II diffractometer facility) at the School of Chemistry, Bharathidasan University. The Council of Scientific and Industrial Research (CSIR), New Delhi is acknowledged for the financial support [Scheme No. 09/475(0154)/2010-EMR-I dated. 09/02/2011] for Senior Research Fellowship to JLP. One of the authors, S.A., thanks for sanction of research schemes, grant number SR/S1/IC-13/2009 of DST, Grant No. 01(2461)/11/EMR-II of CSIR and also Grant No. 41-223/2012(SR) of UGC.

Funding

This work was supported by Council of Scientific and Industrial Research (CSIR), New Delhi [grant number 09/475(0154)/2010-EMR-I], [grant number SR/S1/IC-13/2009], [grant number 01(2461)/11/EMR-II], [grant number 41-223/2012(SR)].

References

[1] Y. Fu, A. Habtemariam, A.M.B.H. Basri, D. Braddick, G.J. Clarkson, P.J. Sadler. *Dalton Trans.*, **40**, 10553 (2011).
[2] T. Boulikas, M. Vougiouka. *Oncol. Rep.*, **10**, 1663 (2003).
[3] E. Wong, C.M. Giandomenico. *Chem. Rev.*, **99**, 2451 (1999).
[4] E.R. Jamieson, S.J. Lippard. *Chem. Rev.*, **99**, 2467 (1999).
[5] T.M. Sielecki, J.F. Boylan, P.A. Benfield, G.L. Trainor. *J. Med. Chem.*, **43**, 1 (2000).
[6] C. Marzano, M. Pellei, F. Tisato, C. Santini. *Anti-Cancer Agents Med. Chem.*, **9**, 185 (2009).
[7] S. Apelgot, J. Coppey, A. Fromentin, E. Guille, M.F. Poupon, A. Roussel. *Anticancer Res.*, **6**, 159 (1986).
[8] S.S. Ranade, V.K. Panday. *Sci. Total Environ.*, **40**, 245 (1984).
[9] D. Jayaraju, A.K. Kondapi. *Curr. Sci.*, **81**, 787 (2001).
[10] M.R. Detty, S.L. Gibson, S.J. Wagner. *J. Med. Chem.*, **47**, 3897 (2004).
[11] M. Ethirajan, Y. Chen, P. Joshi, R.K. Pandey. *Chem. Soc. Rev.*, **40**, 340 (2010).
[12] A.E. O'Connor, W.M. Gallagher, A.T. Byrne. *Photochem. Photobiol.*, **85**, 1053 (2009).
[13] D. Samaroo, M. Vinodu, X. Chen, C.M. Drain. *J. Comb. Chem.*, **9**, 998 (2007).
[14] E.R. Trivedi, A.S. Harney, M.B. Olive, I. Podgorski, K. Moin, B.F. Sloane, A.G.M. Barrett, T.J. Meade, B.M. Hoffman. *Proc. Natl. Acad. Sci. USA*, **107**, 1284 (2010).
[15] M. Mitsunaga, T. Nakajima, K. Sano, P.L. Choyke, H. Kobayashi. *Bioconjugate Chem.*, **23**, 604 (2012).
[16] K. Stefflova, H. Li, J. Chen, G. Zheng. *Bioconjugate Chem.*, **18**, 379 (2007).
[17] D. Crespy, K. Landfester, U.S. Schubert, A. Schiller. *Chem. Commun.*, **46**, 6651 (2010).

[18] M. Harlos, I. Ott, R. Gust, H. Alborzinia, S. Wölfl, A. Kromm, W.S. Sheldrick. *J. Med. Chem.*, **51**, 3924 (2008).
[19] S.L.H. Higgins, A.J. Tucker, B.S.J. Winkel, K.J. Brewer. *Chem. Commun.*, **48**, 67 (2011).
[20] S. Saha, D. Mallick, R. Majumdar, M. Roy, R.R. Dighe, E.D. Jemmis, A.R. Chakravarty. *Inorg. Chem.*, **50**, 2975 (2011).
[21] G.M. Hill, D.M. Moriarity, W.N. Setzer. *Sci. Pharm.*, **79**, 729 (2011).
[22] J.G. Collins, A.D. Sleeman, J.R. Aldrich-Wright, I. Greguric, T.W. Hambley. *Inorg. Chem.*, **37**, 3133 (1998).
[23] M.R. Waterland, K.C. Gordon, J.J. McGarvey, P.M. Jayaweera. *J. Chem. Soc., Dalton Trans.*, 609 (1998).
[24] J. Marmur. *J. Mol. Biol.*, **3**, 208 (1961).
[25] F.H. Allen, W.D. Samuel Motherwell, P.R. Raithby, G.P. Shields, R. Taylor. *New J. Chem.*, **23**, 25 (1999).
[26] G.M. Sheldrick. *Acta Crystallogr. Sect. A: Found. Crystallogr.*, **64**, 112 (2008).
[27] Bruker-Nonius. *APEX-II and SAINT-Plus (Version 7.06a)*, Bruker AXS Inc., Madison, WI (2004).
[28] M.J. Frisch, G.W. Trucks, H.B. Schlegel, G.E. Scuseria, M.A. Robb, J.R. Cheeseman, G. Scalmani, V. Barone, B. Mennucci, G.A. Petersson, H. Nakatsuji, M. Caricato, X. Li, H.P. Hratchian, A.F. Izmaylov, J. Bloino, G. Zheng, J.L. Sonnenberg, M. Hada, M. Ehara, K. Toyota, R. Fukuda, J. Hasegawa, M. Ishida, T. Nakajima, Y. Honda, O. Kitao, H. Nakai, T. Vreven, J.A. Montgomery Jr., J.E. Peralta, F. Ogliaro, M. Bearpark, J.J. Heyd, E. Brothers, K.N. Kudin, V.N. Staroverov, R. Kobayashi, J. Normand, K. Raghavachari, A. Rendell, J.C. Burant, S.S. Iyengar, J. Tomasi, M. Cossi, N. Rega, J.M. Millam, M. Klene, J.E. Knox, J.B. Cross, V. Bakken, C. Adamo, J. Jaramillo, R. Gomperts, R.E. Stratmann, O. Yazyev, A.J. Austin, R. Cammi, C. Pomelli, J.W. Ochterski, R.L. Martin, K. Morokuma, V.G. Zakrzewski, G.A. Voth, P. Salvador, J.J. Dannenberg, S. Dapprich, A.D. Daniels, Ö. Farkas, J.B. Foresman, J.V. Ortiz, J. Cioslowski, D.J. Fox. Gaussian Inc, Wallingford, CT (2009).
[29] D. Mustard, D.W. Ritchie. *Proteins: Struct., Funct., Bioinf.*, **60**, 269 (2005).
[30] Z.B. Ou, Y.H. Lu, Y.M. Lu, S. Chen, Y.H. Xiong, X.H. Zhou, Z.W. Mao, X.Y. Le. *J. Coord. Chem.*, **66**, 2152 (2013).
[31] T.-T. Xing, S.-H. Zhan, Y.-T. Li, Z.-Y. Wu, C.-W. Yan. *J. Coord. Chem.*, **66**, 3149 (2013).
[32] S. Anbu, A. Killivalavan, E.C.B.A. Alegria, G. Mathan, M. Kandaswamy. *J. Coord. Chem.*, **66**, 3989 (2013).
[33] M.-L. Liu, M. Jiang, K. Zheng, Y.-T. Li, Z.-Y. Wu, C.-W. Yan. *J. Coord. Chem.*, **67**, 630 (2014).
[34] A.W. Addison, T.N. Rao, J. Reedijk, J. van Rijn, G.C. Verschoor. *J. Chem. Soc. Dalton Trans.*, 1349 (1984).
[35] R.C. Santra, K. Sengupta, R. Dey, T. Shireen, P. Das, P.S. Guin, K. Mukhopadhyay, S. Das. *J. Coord. Chem.*, **67**, 265 (2014).
[36] A.A. Schilt, R.C. Taylor. *J. Inorg. Nucl. Chem.*, **9**, 211 (1959).
[37] W.P. Griffith, S.I. Mostafa. *Polyhedron*, **11**, 2997 (1992).
[38] L.A. Lipscomb, F.X. Zhou, S.R. Presnell, R.J. Woo, M.E. Peek, R.R. Plaskon, L.D. Williams. *Biochemistry*, **35**, 2818 (1983).
[39] A. Wolfe, G.H. Shimer Jr., T. Meehan. *Biochemistry*, **26**, 6392 (1987).
[40] M. Cory, D.D. McKee, J. Kagan, D.W. Henry, J.A. Miller. *J. Am. Chem. Soc.*, **107**, 2528 (1985).
[41] M.J. Waring. *J. Mol. Biol.*, **13**, 269 (1965).
[42] C.-Z. Xie, M.-M. Sun, S.-H. Li, X.-T. Zhang, X. Qiao, Y. Ouyang, J.-Y. Xu. *J. Coord. Chem.*, **66**, 3891 (2013).
[43] S. Arounaguiri, B.G. Maiya. *Inorg. Chem.*, **35**, 4267 (1996).
[44] J.G. Liu, B.H. Ye, H. Li, L.N. Ji, R.H. Li, J.Y. Zhou. *J. Inorg. Biochem.*, **73**, 117 (1999).
[45] P.R. Reddy, A. Shilpa. *Chem. Biodiver.*, **8**, 1245 (2011).
[46] C.-Y. Zhou, X. Li, Y. Pin. *Biochemistry (Moscow)*, **72**, 27 (2007).
[47] B.C. Baguley, M. Le Bret. *Biochemistry*, **23**, 937 (1984).
[48] B.C. Baguley, M. Le Bret. *Biochemistry*, **12**, 4161 (1973).
[49] S. Mahadevan, M. Palaniandavar. *Inorg. Chem.*, **37**, 693 (1998).
[50] S. Schäfer, I. Ott, R. Gust, W.S. Sheldrick. *Eur. J. Inorg. Chem.*, **2007**, 3034 (2007).
[51] H. Xu, K.C. Zheng, Y. Chen, Y.Z. Li, L.J. Lin, H. Li, P.X. Zhang, L.N. Ji. *J. Chem. Soc., Dalton Trans.*, 2260 (2003).
[52] S. Satyanarayana, J.C. Dabrowiak, J.B. Chaires. *Biochemistry*, **31**, 9319 (1992).